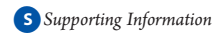
pubs.acs.org/JPCC

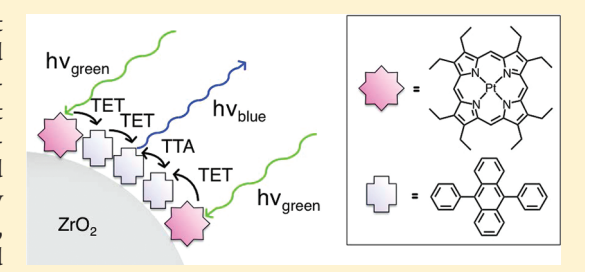
Photon Upconversion on Dye-Sensitized Nanostructured ZrO₂ Films

Jonas Sandby Lissau, James M. Gardner, and Ana Morandeira*

Department of Photochemistry and Molecular Science, Uppsala University, Box 523, SE-75120 Uppsala, Sweden



ABSTRACT: Photon upconversion based on sensitized triplet—triplet annihilation has been observed on nanocrystalline ZrO_2 films cosensitized with platinum(II) octaethylporphyrin (triplet sensitizer) and 9,10-diphenylanthracene (singlet emitter) under sunlight-like conditions (noncoherent excitation source, excitation light intensity as low as 5 mW/cm²). Timeresolved emission measurements showed a fast rise of the upconverted signal (\leq 10 ns), suggesting that triplet energy migration most probably occurs through a "static" Dexter mechanism. To the best of our knowledge, this is the first observation of photon upconversion based on sensitized triplet—triplet annihilation on a sensitized mesoporous metal oxide.



Implementation of similar systems in dye-sensitized solar cells would increase the maximum theoretical efficiency of these devices from 30% to over 40%.

1. INTRODUCTION

Investigation of photon upconversion based on sensitized triplet—triplet annihilation (UC-STTA) has experienced a strong resurgence in the past decade.¹ A main reason behind this renewed interest is the fact that UC-STTA can occur under sunlight-like conditions, namely, low-intensity, noncoherent excitation light,² so that it is potentially useful in photovoltaics.

UC-STTA can be described as follows (see Scheme 1): A sensitizer molecule, *S*, typically an inorganic complex with highly efficient intersystem crossing, absorbs a low-energy photon and stores the excitation energy in a long-lived triplet state

$$S + h\nu_{low} \rightarrow {}^{1}S^{*} \tag{1}$$

$$^{1}S^{*} \rightarrow ^{3}S^{*} \tag{2}$$

The excitation energy is then transferred to the triplet excited state of the emitter molecule, E, commonly an organic compound with a low-lying triplet state and a high-energy excited singlet state, through triplet energy transfer (TET)

$${}^{3}S^{*} + E \rightarrow S + {}^{3}E^{*}$$
 (3)

Encounter of two molecules in their triplet excited states (usually two emitters) can lead to triplet—triplet annihilation (TTA) and formation of the high-energy singlet excited state of an emitter molecule

$${}^{3}E^{*} + {}^{3}E^{*} \rightarrow E + {}^{1}E^{*}$$
 (4)

and in the absence of quenching mechanisms, a delayed high-energy photon is released

$$^{1}E^{*} \rightarrow E + h\nu_{\text{high}}$$
 (5)

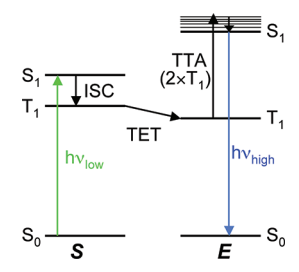
As pointed out by Ekins-Daukes and Schmidt,³ UC-STTA is especially well-suited to be implemented in dye-sensitized solar

cells (DSSCs). A standard DSSC consists of a photoactive anode, typically nanostructured TiO₂ coated with a dye; a counterelectrode; and a mediator, to regenerate the oxidized dye and close the circuit. One could conceive of a DSSC wherein low-energy photons are absorbed by sensitizer molecules and, through the UC-STTA mechanism, produce high-energy excited states in emitter molecules that can inject electrons into TiO₂, thereby converting low-energy photons into high-energy electrons. Common single-threshold solar cells have a theoretical maximum efficiency of 30%. Replacing standard sensitizer dyes by a mixture of sensitizer and emitter dyes, that is, employing a UC-STTA system, would raise the theoretical maximum efficiency to over 40%. This could significantly increase the efficiency of DSSCs, currently stagnant at 12%. 4

Most low-excitation-intensity studies have focused on monitoring UC-STTA in solution or rubbery polymer matrixes,1 where molecular diffusion of the triplet emitters is possible. To the best of our knowledge, no low-excitation-intensity studies of UC-STTA have been carried out on sensitized nanostructured metal oxides, the essential building blocks of DSSCs. This kind of material presents a very different environment than a solution or rubbery polymer matrixes, as emitter and sensitizer dyes are, in principle, anchored to the mesoporous metal oxide surface. Therefore, efficient diffusion of the excitation energy requires energy migration between neighboring molecules. This could be a challenging requirement to meet, because triplet energy transfer between organic molecules will, in principle, involve a pure Dexter mechanism. This mechanism requires orbital overlap between the energy donor and acceptor dyes and, therefore, close proximity. However, it is known that sensitized

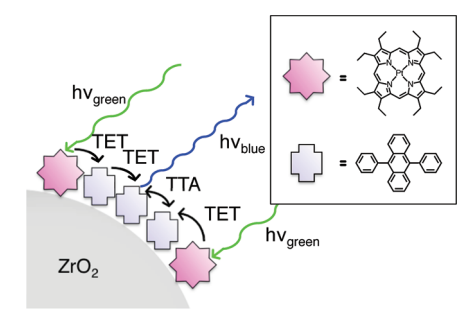
Received: October 11, 2011 **Published:** October 18, 2011

Scheme 1. Processes Involved in Photon Upconversion Based on Sensitized Triplet—Triplet Annihilation (UC-STTA)^{a,b}



 a S, sensitizer; E, emitter; S₀, ground state; S₁, first excited singlet state; T₁, first excited triplet state; ISC, intersystem crossing; TET, triplet energy transfer; TTA, triplet—triplet annihilation. b See text for more details

Scheme 2. Proposed Mechanism for UC-STTA on DPA—PtOEP-Sensitized Nanocrystalline ZrO₂



nanocrystalline metal oxide films or colloids can reach very high local concentrations of dye. These materials can, in fact, enhance intermolecular energy migration, and there are several reports of efficient TET under low excitation intensities involving heavymetal polypyridine complexes and even purely organic dyes. It must be noted, however, that, in the former case, a certain degree of long-range energy transfer (Förster mechanism, also known as Förster resonance energy transfer) can be involved because of spin—orbit coupling.

As a proof of principle to ascertain whether UC-STTA can occur on sensitized nanostructured metal oxides, we initiated fundamental studies on nanocrystalline ZrO2 films cosensitized with the triplet sensitizer platinum(II) octaethylporphyrin (PtOEP) and the singlet emitter 9,10-diphenylanthracene (DPA). This pair of dye molecules was chosen because of their commercial availability and previously reported photon upconversion in solution 10 and in poly(methyl methacrylate) (PMMA) films¹¹ under low excitation light intensities. The surface properties and refractive index of ZrO2 are comparable to those of TiO₂, ¹² but its conduction band is approximately 1.3 eV higher than that of TiO2, 13 thus excluding the possibility of electron injection from the singlet excited emitter into the semiconductor and, therefore, quenching of the upconverted emission. Scheme 2 shows the proposed mechanism for UC-STTA on DPA-PtOEP-sensitized nanocrystalline ZrO2. According to this mechanism, PtOEP sensitizers absorb green photons and transfer the excitation energy to DPA molecules through TET. The energy migrates from DPA molecule to DPA molecule, again through TET, until the encounter of two triplet excited states

leads to TTA and formation of a high-energy singlet excited state. In the absence of quenching mechanisms, a delayed blue photon is released.

2. EXPERIMENTAL SECTION

2.1. Samples. Mesoporous ZrO₂ thin films were prepared by blade-casting, with a glass rod, a homemade dispersion of 12 \pm 3 nm ZrO₂ nanoparticles onto glass microscope slides (Menzel-Gläser) that were masked with a spacer of transparent adhesive tape. The films were allowed to air-dry for approximately 1 h, at which time the tape was removed and the slides were sintered at 450 °C for 30 min using a hot plate programmed for stepwise heating. The resulting films were $4-6 \mu m$ thick. The following sensitization regimens were utilized unless otherwise stated: For ZrO₂ samples that were sensitized only with DPA, the ZrO₂ substrates were dipped for 48 h into a toluene solution (Sigma-Aldrich, spectrophotometric grade) of 20.2 mM DPA (Fluka). For ZrO₂ films cosensitized with DPA and PtOEP, the sensitizing solution was a mixture of 20.3 mM DPA and 0.3 mM PtOEP (Aldrich) in toluene. For steady-state and time-resolved measurements, 0.1 cm \times 0.8 cm \times 2.6 cm pieces of the sensitized substrates were inserted into 0.2 cm \times 1 cm \times 4 cm cuvettes containing water, which were purged with argon for ca. 30 min prior to and during each emission measurement. Water was chosen as a surrounding medium because of its low oxygen concentration and because it minimized the amount of noise in the measurements produced by light scattering and enhanced the physisorption of the highly nonpolar dyes to the ZrO₂ surface.

It is important to mention that the amplitude of the upconverted signal was very sensitive to the sample preparation conditions. Sensitized films with similar dye loadings (absorption spectrum, film thickness) would exhibit very different upconversion efficiencies when prepared with a different ZrO₂ paste or under different humidity conditions. PtOEP dimer formation, which leads to loss of upconversion efficiency (see section 3 for more details), was also strongly dependent on the sample preparation conditions.

- **2.2.** Grazing-Incidence X-ray Diffraction (Gi-XRD). The nanocrystalline $\rm ZrO_2$ films were analyzed by grazing-incidence X-ray diffraction (Gi-XRD) on a Siemens D5000 diffractometer equipped with a parallel beam optics system using a Cu K α X-ray radiation source. The angle of incidence was fixed at 3°. Applying the Scherrer equation, ¹⁴ we obtained a mean size of 12 \pm 3 nm for the $\rm ZrO_2$ nanoparticles. See Figure S1 in the Supporting Information for a typical diffractogram and its analysis.
- **2.3. Steady-State Absorption Measurements.** A double-beam Cary 5000 spectrophotometer (Varian) was used to record steady-state absorption spectra. Special care was taken to minimize the amount of scattered light reaching the detector. Because it was not possible to completely avoid the presence of scattered light, we used "background modeling" to subtract the scattering component from the absorption spectra, as described in the literature. ¹⁵ Igor Pro software was used to carry out the least-squares fit. See Figure S2 in the Supporting Information for a typical absorption spectrum of a DPA-sensitized ZrO₂ film before and after application of the correction.
- **2.4. Steady-State Emission Measurements.** Standard steady-state emission spectra were obtained on a Fluorolog-3 instrument (Horiba Jobin Yvon) equipped with double-grating excitation and emission monochromators and a 450-W Xe lamp as a light source. The emission spectra were corrected for the

spectral sensitivity of the detection system by using a calibration file of the detector response. Background corrections were performed by using a nanostructured $\rm ZrO_2$ film as a blank. The blank films were always cut from the same microscope slide as the films used for the sensitized samples. Front-face illumination (30° with respect to the incident beam) was used to minimize inner-filter effects.

For upconverted emission measurements, the excitation and emission slits were set to obtain 10- and 4-nm bandpasses, respectively, and an integration of 4 s per point. A 400-nm long-pass filter was placed in front of the sample to eliminate second-order diffraction by the excitation monochromator. In these conditions, the excitation light intensity was 8 mW/cm². This is of the same order of magnitude as the intensity of the sunlight in the PtOEP Q-band range. ¹⁶

To study the dependence of the photon upconversion on the incident light power, the power was varied by placing different combinations of neutral-density filters and/or coverslips between the light source (Xe lamp) and the sample. A high-sensitivity silicon sensor (LM-2 Vis, Coherent) coupled to a power meter (FieldMaster-GS, Coherent) was used to monitor the incident light power. The spectra were background-corrected.

2.5. Time-Resolved Emission Measurements. Time-resolved emission measurements were performed in the following way: A frequency-tripled Q-switched Nd:YAG laser (Quanta-Ray PRO Series-230, Spectra-Physics) was used to pump an optical parametric oscillator (Quanta-Ray MOPO-710, Spectra-Physics) to produce 536-nm, 10-ns laser pulses at a repetition rate of 10 Hz. The excitation light intensity was adjusted to 2.5 mJ/cm² per pulse using a metallic mesh. The samples were oriented by approximately 30° with respect to the excitation beam. The resultant emission was collected at 90° from the excitation source. The detection system was composed of a monochromator (Edinburgh Instruments) and an intensified charge-coupled device (iCCD) camera (Andor DH720). The signal was processed with Edinburgh Instruments L900 software. A Schott BG12 glass filter was used to minimize the amount of excitation scattered light reaching the detector. The presence of this filter slightly distorted the red edge of the DPA singlet emission spectrum.

3. RESULTS AND DISCUSSION

3.1. Steady-State Characterization. Figure 1a shows the steady-state absorption and emission spectra of DPA and PtOEP ($\lambda_{\rm exc}$ = 393 and 536 nm, respectively) at low concentrations in toluene. Figure 1b shows similar spectra for only DPA and DPA—PtOEP-sensitized ZrO₂. As can be seen in the spectra, selective excitation of PtOEP and subsequent detection of DPA emission is possible, meaning that UC-STTA can be detected by steady-state methods. The changes in the absorption and emission spectra of DPA upon adsorption are relatively small, mainly a 4-nm bathochromic shift (the disappearance of the high-energy vibronic peak in the DPA-adsorbed emission spectrum is due to an inner-filter effect). This indicates that there is no strong interaction between DPA molecules when adsorbed onto ZrO₂ and allows the presence of aggregates to be excluded.

From a basic surface coverage calculation, the concentration of DPA on a $\rm ZrO_2$ nanoparticle surface was found to be less than 10% of a monolayer. Briefly, the surface coverage of DPA on $\rm ZrO_2$ was calculated by utilizing absorption data for DPA on $\rm ZrO_2$, the measured film thickness, and a uniform particle size of 12 nm.

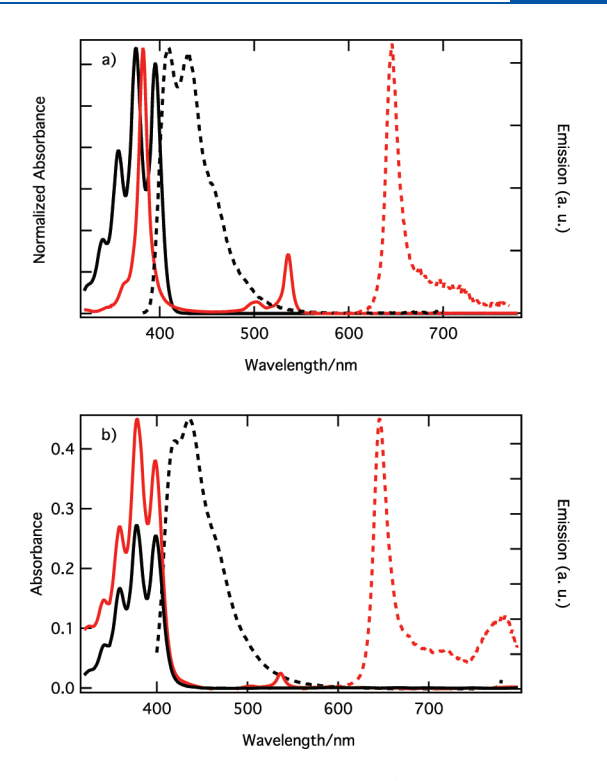


Figure 1. Steady-state absorption (solid lines) and corrected emission (dashed lines) spectra of (a) DPA (black, $\lambda_{\rm exc} = 393$ nm) and PtOEP (red, $\lambda_{\rm exc} = 536$ nm) in dilute toluene solution and (b) DPA- (black, $\lambda_{\rm exc} = 393$ nm) and DPA-PtOEP- (red, $\lambda_{\rm exc} = 536$ nm) sensitized ZrO₂ nanocrystalline films in water. The thicknesses of the films were 5.6 and 5.3 μ m, respectively. The absorption spectra measured on films were analytically corrected for the scattering of the samples (see the text and the Supporting Information).

It was assumed that the porosity was 50% for a mesoporous $\rm ZrO_2$ thin film, that the DPA dye molecules lay flat on the $\rm ZrO_2$ surface, and that the DPA surface distribution was uniform. This relatively low coverage agrees well with the fact that interaction between DPA molecules appears to be insignificant.

The effect on the absorption and emission spectra of PtOEP adsorption was somewhat greater. Careful analysis of the absorption spectra shows a slight broadening of the Soret band and a small decrease of the Soret band-to-Q-band intensity ratio. This is a good indication of an increase in coupling between PtOEP molecules. Further evidence is provided by the presence of an additional emission band around 780 nm, assigned to PtOEP dimer phosphorescence. However, the predominance of the monomer emission band, at 645 nm, indicates that the presence of PtOEP dimers is relatively low.

It is notable that binding of PtOEP onto a ZrO₂ film in the absence of DPA led to significant aggregation of PtOEP and a dominant dimer emission; see the Supporting Information. The simplest possible explanation for this observation is that an association complex between DPA and PtOEP forms in solution that prevents PtOEP from associating with itself and, therefore, prevents aggregation. Anecdotally, this could indicate that close contact between PtOEP and DPA starts in solution and is maintained on the surface of ZrO₂ as well.

3.2. Photon Upconverted Emission. Excitation of DPA—PtOEP-sensitized ZrO_2 films at the Q-band of PtOEP (536 nm) also yields an anti-Stokes emission band with maximum intensity at 436 nm (see Figure 2). The observed emission is in excellent

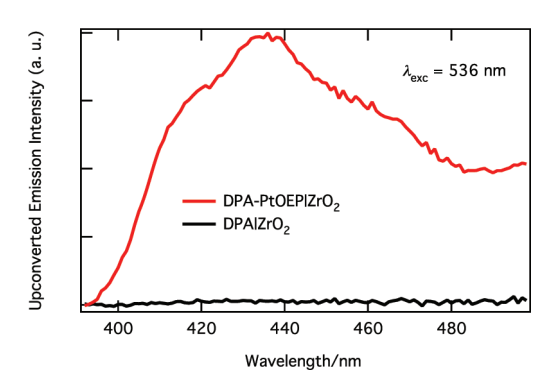


Figure 2. (Red) Steady-state upconverted emission spectrum of DPA–PtOEP|ZrO₂ in water ($\lambda_{\rm exc}$ = 536 nm, incident power density = 8 mW/cm²). (Black) Emission spectrum of DPA|ZrO₂ in water measured under identical conditions.

agreement with the prompt fluorescence spectrum of DPA adsorbed upon $\rm ZrO_2$ (compare Figures 2 and 1b). No anti-Stokes emission was observed upon 536-nm excitation of $\rm ZrO_2$ samples sensitized with only DPA. Therefore, we assign the observed anti-Stokes emission to UC-STTA.

As observed in solution and other solid-state host systems reported previously, the magnitude of the photon upconverted emission was strongly dependent on the absolute and relative concentrations of sensitizer and emitter dyes. Optimization of the sensitizer and emitter concentrations was done by varying different sensitization parameters such as the sensitization time (from 3 h to 6 days), emitter concentration (from 2.6 to 20.6 mM), and sensitizer concentration (from 0.1 to 2.6 mM) and measuring the amplitude of the upconverted signal. The upconverted signal was found to peak when the films were dipped for 48 h in a mixture of 20.3 mM DPA (close to the dye saturation limit) and 0.3 mM PtOEP in toluene.

The cosensitized samples showed photodegradation, especially in the presence of oxygen. Therefore, special care was taken to purge the samples with Ar for ca. 30 min prior to and during each measurement. Longer purging times did not have a significant effect on the amplitude of the signal. Freshly prepared samples were used for each individual upconverted emission measurement. The quenching of the signal in the presence of air or nondeoxygenated water further supports its assignment to UC-STTA, because oxygen is a well-known quencher of triplet excited states. One example of particular relevance to our study is the direct observation of triplet-state quenching by oxygen in a DPA/PtOEP system in solution by Monguzzi et al. ¹⁸

3.3. Photon Upconversion Dependence on Incident Light Power. The magnitude of the photon upconversion signal was monitored at different incident light intensities, ranging from 4.6 to 7.6 mW/cm² (Figure 3a). The range of excitation intensities is rather narrow, limited by the intensity of the Xe lamp (upper limit) and the small amplitude of the monitored signal (lower limit). To minimize the light exposure of the sample and thus its photodegradation, the measurements were carried out from low to high values of the light power and with a large interval between points (7 nm). Because the amplitude of the upconverted signals was small and the nanostructured samples were highly scattering (see, for instance, the red edge of the spectrum shown in Figure 2), the spectra were collected only up to 460 nm. In this way, the contribution of incident scattered light to the observed emission was kept to a minimum.

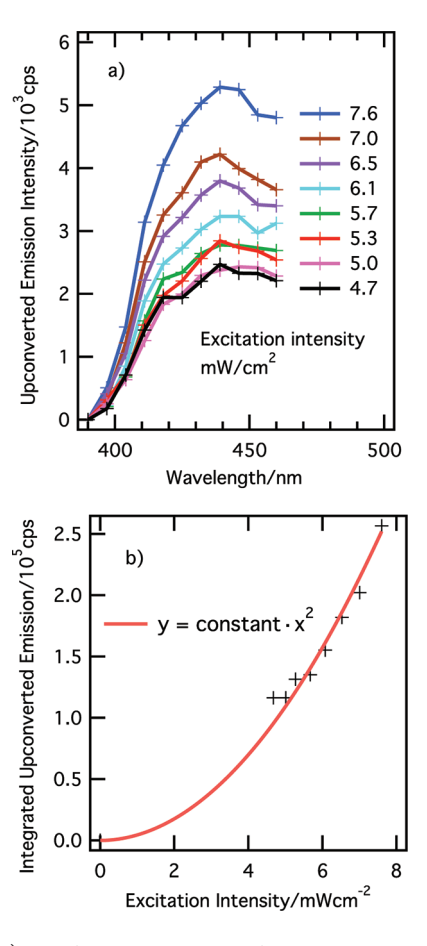


Figure 3. (a) Steady-state upconverted emission spectra of DPA—PtOEP|ZrO $_2$ in water ($\lambda_{\rm exc}=536$ nm) at different incident power densities. The spectra were recorded with a large interval between points and over a narrow range to minimize sample photodegradation and contribution from scattered excitation light. (b) Integrated emission of the spectra presented in a (black crosses) versus the incident power density and the best quadratic fit to the data (red solid line). See text for more details.

Figure 3b shows the integrated emission of the spectra presented in Figure 3a (black crosses) as a function of the incident power density and the best quadratic fit to the data (red solid line). The integrated upconverted emission is proportional to the square of the power density. Such nonlinear dependence is expected in processes involving TTA. 19 Similar behavior has previously been observed in UC-STTA studies at similar excitation intensities of other solid-state systems such as rubbery polymer blends⁵ and rigid polymer films.¹¹ It is important to note, however, that the upconverted emission of DPA-PtOEP|ZrO₂ samples does not always follow a perfectly quadratic dependence on the incident power density. Higher power dependences have been observed in otherwise similar samples (see the Supporting Information). This cannot be attributed to simultaneous photon absorption²⁰ because the samples were excited with a noncoherent source, at very low intensities. At the moment, it is not clear whether the observation is due to the small magnitude of the monitored signals (and therefore to the error associated with the measurements) or a more fundamental cause. However, despite the experimental uncertainties, there is no doubt that the upconverted signal exhibits a higher-than-linear dependence on the excitation intensity.

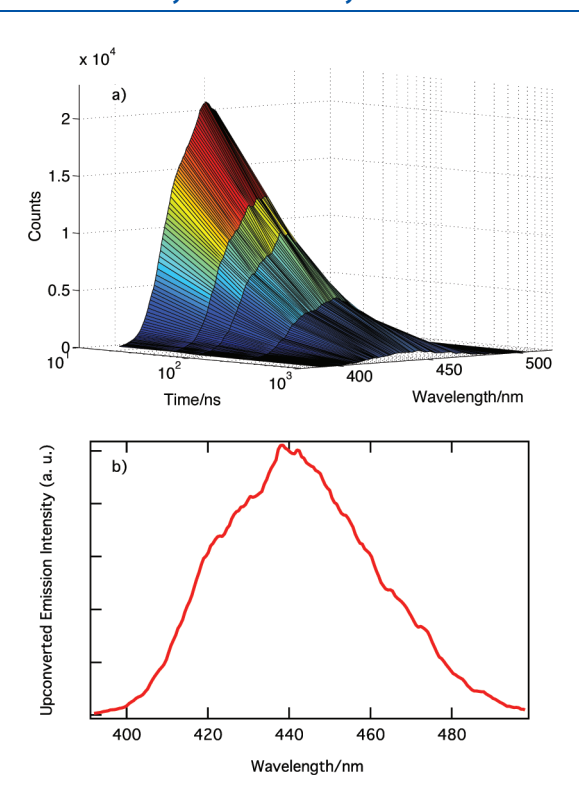


Figure 4. (a) Spectral decay of the upconverted emission of DPA–PtOEP|ZrO₂ in water ($\lambda_{\text{exc}} = 536 \text{ nm}$).²³ (b) Slice at 75 ns.

3.4. Time-Resolved Emission Measurements. Figure 4a shows the anti-Stokes emission decay of a DPA-PtOEP-sensitized ZrO_2 sample after excitation of the PtOEP sensitizer (λ_{exc} = 536 nm). The observed emission matches the fluorescence spectrum of DPA very well (compare Figure 4b and Figure 1b). Although the limited number of data points excludes the possibility of a rigorous analysis, the emission decay is clearly nonexponential with a half-life of about 75 ns. Taking into account that the singlet excited-state lifetime of DPA is 8 ns in solution, ²¹ the relatively slow decay of the observed signal is further evidence that we were monitoring DPA delayed fluorescence (UC-STTA) as opposed to prompt fluorescence. The rise of the upconverted emission was faster than the time resolution of our experiment, \sim 10 ns. This is a good indication that the involved TET and TTA mechanisms must be prevalently "static"; that is, surface diffusion of the sensitizer or emitter dye molecules does not seem to play a significant role.²²

3.5. Photon Upconversion Quantum Yield. The efficiency of UC-STTA is strongly dependent on several factors such as excitation energy (as discussed above, the upconverted signal has a nonlinear dependence on the incident power density), absolute and relative concentrations of sensitizer and emitter dyes, the medium (viscous or fluid, liquid or solid), and temperature. For this reason UC-STTA quantum yields are always reported for very specific, well-defined conditions. In our case, the efficiency of the UC-STTA process was estimated using the fluorescence intensity of directly excited DPA as an internal reference; that is

$$\Phi_{\text{UC-STTA}} = 2c\Phi_{\text{DPA}} \frac{I_c(\lambda_{\text{exc}} = 536\text{nm})}{I_c(\lambda_{\text{exc}} = 393\text{nm})} \frac{\text{LHE}(\lambda_{\text{exc}} = 393\text{nm})}{\text{LHE}(\lambda_{\text{exc}} = 536\text{nm})}$$
(6)

where $\Phi_{\text{UC-STTA}}$ is the UC-STTA quantum yield. Φ_{DPA} is the fluorescence quantum yield of directly excited DPA. I_c corresponds

to the DPA emission intensity due to direct excitation of the dye ($\lambda_{\rm exc}$ = 393 nm) or UC-STTA ($\lambda_{\rm exc}$ = 536 nm), corrected to account for the different intensity of the Xe lamp at the excitation wavelengths. LHE(λ) is the light-harvesting efficiency of the sample at the excitation wavelength

$$LHE(\lambda) = 1 - 10^{-A(\lambda)} \tag{7}$$

The factor 2 accounts for the fact that two absorbed photons are required to produce one upconverted photon. Finally, the factor c introduces a correction for the different experimental conditions under which the measurements were performed, such as slit width and integration time. ²⁴ Both emission measurements were carried out on the same sample; therefore, there is no need to account for the refractive index of the medium.

Applying eq 6 to the steady-state upconversion emission measurements presented in section 3.2 and assuming that the quantum yield of fluorescence of DPA adsorbed onto $\rm ZrO_2$ is the same as in solution $(\Phi_{\rm DPA}=0.93),^{25}$ a quantum yield of (6 \times 10 $^{-4}$)% was obtained for the DPA upconverted emission of a DPA—PtOEP-sensitized mesoporous $\rm ZrO_2$ film in water, excited at 536 nm (10-nm bandpass) with a power density of 8 mW/cm² at room temperature. The steady-state absorption spectrum of the sample, which reflects the absolute and relative concentrations of the emitter and sensitizer dyes, is shown in Figure 1b (solid red line).

In addition to the upconversion quantum yield, we also estimated the quantum yield of TET from PtOEP to DPA, the first intermolecular step of the UC-STTA process. The estimate was based on a comparison of PtOEP excited-state lifetimes in the absence and presence of DPA. The calculated efficiency is reasonably high and indicates that this first energy-transfer step is not limiting the upconversion efficiency (see the Supporting Information for more details).

Several literature reports in recent years have remarked on the fact that UC-STTA is significantly less efficient in solid-state host materials than in solution. The observation has generally been attributed to the lower mobility of the excited emitter and sensitizer dye molecules in the solid state. 5,26 To our knowledge, there is only one report of the quantum yield of UC-STTA in a solid matrix under noncoherent, low-excitation-energy conditions. 11 In that case, the authors studied the upconversion efficiency of a DPA (emitter)/PtOEP (sensitizer) blend in a rigid polymer (PMMA) under ultralow excitation energy (0.9 mW/cm², noncoherent excitation source). As in our work, the quantum efficiency was calculated by comparison with the emission intensity of the directly excited DPA. Despite the very low excitation energies used and the rigidity of the matrix precluding molecular diffusion of the triplet emitters, a respectable quantum efficiency of 0.02% was measured. This is about 30 times larger than the UC-STTA quantum yield measured in our system. Although the aim of our work was, as a proof of principle, to ascertain whether UC-STTA could occur on sensitized nanostructured metal oxides, not to obtain a highly efficient photon upconverting system, it is nevertheless interesting to discuss the possible reasons for the low quantum yield.

First, a significant difference between the systems is that, even though the same sensitizer/emitter couple was used, the DPA/PtOEP blend in PMMA was unaffected by the presence of oxygen, whereas the DPA—PtOEP|ZrO₂ films were rather sensitive to photodegradation, which was enhanced in the presence of oxygen. Therefore, a reasonable assumption is that the

concentration of molecular oxygen in the PMMA matrix is lower and/or the oxygen is less "mobile" than that on sensitized $\rm ZrO_2$, even after purging with Ar. Preparing sealed samples in an anaerobic environment, such as a glovebox, would circumvent this problem.

A second aspect to consider is the formation of PtOEP dimers, which leads to a loss of upconversion efficiency. PtOEP appears to show good solubility in PMMA, with no formation of dimers. ¹¹ In the case of sensitized ZrO₂, it was not possible to completely eliminate the formation of dimers, and even the best upconverting samples showed a small amount of triplet emission from PtOEP dimers (see Figure 1b).

Finally, the molecular orientation of adjacent DPA molecules on the surface of $\rm ZrO_2$ might be unfavorable for TET. Dexter energy transfer relies on strong overlap between the orbitals of the involved molecules. Because of the polarity of the surrounding solvent (water) and the hydrophobicity of DPA, it is likely that DPA lies flat against the $\rm ZrO_2$ surface; it is coplanar. The coplanar orientation can cause weak orbital overlap between adjacent DPA molecules and prevent efficient energy migration. This problem should be less relevant in the PMMA matrix because of the random orientation of the dye molecules.

Therefore, a possible way to improve the efficiency of UC-STTA on sensitized nanostructured metal oxides would be to introduce anchoring groups on the dye molecules that would allow for optimization of the orientations of the dye molecules, giving rise to less dimer formation and better orbital overlap. Moreover, because the surface coverage of DPA is less than 10% of a monolayer, the introduction of binding groups onto DPA could give better control of the molecular spacing, increase the emitter dye loading, decrease the space between adjacent molecules, and improve the orbital overlap.

4. SUMMARY

Herein, we have reported on the observation of photon upconversion based on sensitized triplet—triplet annihilation (UC-STTA) on DPA—PtOEP-sensitized nanostructured ZrO₂ at excitation light intensities as low as 5 mW/cm² using a noncoherent excitation source. A nonlinear (quadratic or higher) dependence of the upconverted signal on the incident light power density was observed, which reinforces the proposed mechanism. Time-resolved measurements pointed to TET through a static Dexter mechanism. The quantum yield of the upconversion process was low, probably because of the unfavorable orientation of the adsorbed DPA (emitter) molecules on the ZrO₂ surface. Further work is planned to address this issue through the introduction of anchoring groups on the dye molecules.

To the best of our knowledge, this is the first observation of UC-STTA on a sensitized mesoporous metal oxide. The work herein could guide the use of UC-STTA systems to increase the theoretical efficiency of DSSCs to greater than 40%.

ASSOCIATED CONTENT

Supporting Information. ZrO₂ diffractogram. Analytical subtraction of the scattering component from the films' absorption spectra. Additional measurement of the dependence of the upconverted signal on the incident light power. Time-resolved PtOEP emission decay. This material is available free of charge via the Internet at http://pubs.acs.org.

AUTHOR INFORMATION

Corresponding Author

*E-mail: Ana.Morandeira@fotomol.uu.se.

ACKNOWLEDGMENT

We thank B. O'Regan (Imperial College London, UK) for providing us with the recipe to prepare colloidal ZrO₂ and L. Häggman (Uppsala University, Sweden) for his help in the preparation of the paste. AM thanks N. J. Ekins-Daukes (Imperial College London, UK) and T. W. Schmidt (The University of Sydney, Australia) for stimulating and inspiring discussions. JL thanks the foundation Futura for a traveling scholarship. This work was supported by the Swedish Research Council (VR) and the Knut and Alice Wallenberg Foundation.

REFERENCES

- (1) Singh-Rachford, T. N.; Castellano, F. N. Coord. Chem. Rev. 2010, 254, 2560–2573.
- (2) Baluschev, S.; Yakutkin, V.; Miteva, T.; Avlasevich, Y.; Chernov, S.; Aleshchenkov, S.; Nelles, G.; Cheprakov, A.; Yasuda, A.; Müllen, K.; Wegner, G. *Angew. Chem., Int. Ed.* **2007**, *46*, 7693–7696.
- (3) Ekins-Daukes, N. J.; Schmidt, T. W. Appl. Phys. Lett. 2008, 93, 063507.
- (4) Hagfeldt, A.; Boschloo, G.; Sun, L.; Kloo, L.; Pettersson, H. Chem. Rev. 2010, 110, 6595–6663.
- (5) (a) Islangulov, R. R.; Lott, J.; Weder, C.; Castellano, F. N. J. Am. Chem. Soc. 2007, 129, 12652–12653. (b) Singh-Rachford, T. N.; Lott, J.; Weder, C.; Castellano, F. N. J. Am. Chem. Soc. 2009, 131, 12007–12014.
 - (6) Dexter, D. L. J. Chem. Phys. 1953, 21, 836-850.
- (7) (a) Hoertz, P. G.; Carlisle, R. A.; Meyer, G. J.; Wang, D.; Piotrowiak, P.; Galoppini, E. *Nano Lett.* **2003**, *3*, 325–330. (b) Thyagarajan, S.; Galoppini, E.; Persson, P.; Giaimuccio, J. M.; Meyer, G. J. *Langmuir* **2009**, 25, 9219–9226.
- (8) (a) Higgins, G. T.; Bergeron, B. V.; Hasselmann, G. M.; Farzad, F.; Meyer, G. J. *J. Phys. Chem. B* **2006**, *110*, 2598–2605. (b) Trammell, S. A.; Yang, J.; Sykora, M.; Fleming, C. N.; Odobel, F.; Meyer, T. J. *J. Phys. Chem. B* **2001**, *105*, 8895–8904.
 - (9) Kamat, P. V.; Ford, W. E. Chem. Phys. Lett. 1987, 135, 421-426.
- (10) Monguzzi, A.; Mezyk, J.; Scotognella, F.; Tubino, R.; Meinardi, F. *Phys. Rev. B* **2008**, *78*, 195112.
 - (11) Merkel, P. B.; Dinnocenzo, J. P. J. Lumin. 2009, 129, 303–306.
- (12) Kay, A.; Humphry-Baker, R.; Grätzel, M. J. Phys. Chem. 1994, 98, 952–959.
- (13) Giaimuccio, J. M.; Rowley, J. G.; Meyer, G. J.; Wang, D.; Galoppini, E. Chem. Phys. **2007**, 339, 146–153.
 - (14) Patterson, A. L. Phys. Rev. 1939, 56, 978–982.
- (15) Owen, T. Fundamentals of UV-Visible Spectroscopy. A Workbook; Hewlett-Packard, 1996.
- (16) AM 1.5 G solar radiation spectrum. Integration over the low-energy vibronic band of the porphyrin Q-band yields a solar irradiance of 4 mW/cm^2 .
- (17) Kalinowski, J.; Stampor, W.; Szmytkowski, J.; Cocchi, M.; Virgili, D.; Fattori, V.; Di Marco, P. J. Chem. Phys. 2005, 122, 154710.
- (18) Monguzzi, A.; Tubino, R.; Salamone, M. M.; Meinardi, F. *Phys. Rev. B* **2010**, *82*, 125113.
- (19) Parker, C. A. Photoluminescence of Solutions; Elsevier Publishing Company: Amsterdam, 1968.
- (20) Singh-Rachford, T. N.; Castellano, F. N. J. Phys. Chem. A 2009, 113, 9266–9269.
- (21) Murov, S. L.; Carmichael, I.; Hug, G. L. Handbook of Photochemistry, 2nd ed.; Marcel Dekker, Inc.: New York, 1993.
- (22) Turro, N. J.; Zimmt, M. B.; Gould, I. R.; Mahler, W. J. Am. Chem. Soc. 1985, 107, 5826–5827.

- (23) The monochromator controlled by the iCCD camera was set to a bandpass of 5 nm. The sampling width of each spectrum was 30 ns. Between 30 and 50 measurements were made and averaged per spectrum. Each spectrum was smoothed with a built-in MATLAB procedure.
- (24) The magnitudes of the signals were so different that narrower monochromator slits and shorter integration times were required in the case of direct excitation of DPA to avoid saturation of the emission detector. To calculate the factor c, a very dilute solution of Ru(bpy)₃Cl₂ in water was measured under the conditions (bandpass, integration time) described for direct excitation and upconversion emission of DPA. It was found that the collected emission was 6500 times larger using the upconversion experimental setup.
 - (25) Meech, S. R.; Phillips, D. J. Photochem. 1983, 23, 193-217.
- (26) Monguzzi, A.; Tubino, R.; Meinardi, F. J. Phys. Chem. A 2009, 113, 1171–1174.